Received: 24 February 2024 | Revised: 19 March 2024 | Accepted: 22 March 2024

DOI: 10.1002/jsid.1298

WILEY

SPECIAL SECTION PAPER

High-efficiency and ultracompact pancake optics for virtual reality

Yuqiang Ding, SID Student Member[1] | **Zhenyi Luo, SID Student Member**[1] | **Garimagai Borjigin, SID Member**[1,2,3] | **Shin-Tson Wu, SID Fellow**[1]

[1]College of Optics and Photonics, University of Central Florida, Orlando, Florida, USA

[2]Department of Intelligent Interaction Technologies, University of Tsukuba, Tsukuba, Ibaraki, Japan

[3]Research Fellow of Japan Society for the Promotion of Science, Chiyoda-ku, Tokyo, Japan

Correspondence
Shin-Tson Wu, College of Optics and Photonics, University of Central Florida, Orlando, FL 32816, USA.
Email: swu@creol.ucf.edu

Abstract

Pancake lens has been widely used in virtual reality (VR) and mixed reality (MR) due to its compact form factor. However, using a half mirror (HM) to fold the optical path results in a tremendous optical loss. To enhance the optical efficiency while keeping a compact form factor, we present a new folded optical system incorporating a nonreciprocal polarization rotator. In our proof-of-concept experiment using a commercial Faraday rotator (FR), the theoretically predicted 100% efficiency is validated. Besides, the angular response of terbium gallium garnet (TGG) material is simulated for the first time and the results indicate that such an FR is relatively insensitive to the incident angle, which can dramatically enhance the contrast ratio of our pancake design. Finally, the potential application of such pancake optics for ultracompact near-infrared (NIR) night vision goggles is also discussed.

KEYWORDS

night vision goggle, nonreciprocal polarization rotator, pancake optics, virtual reality

1 | INTRODUCTION

The advent of augmented reality (AR) and virtual reality (VR) has dramatically broadened our perceptual boundaries, catalyzing profound human-digital engagements that surpass the limitations of conventional flat panel displays. This transformative progression has opened a realm of thrilling opportunities, embracing concepts like the metaverse, digital twins, and spatial computing, all of which have permeated various sectors including education, healthcare, navigation, gaming, entertainment, and manufacturing.

To ensure the widespread adoption of AR and VR as wearable technologies over extended durations, it is imperative to prioritize factors such as compactness, style, lightweight design, and low power consumption. Extensive research endeavors[1–3] have been directed toward the development of innovative optical components and headset configurations to meet these objectives. Notably, polarization-based folded optics, commonly known as pancake optics, have emerged as a groundbreaking solution for creating compact and lightweight VR headsets. Examples include products like Apple Vision Pro and Meta Quest Pro,[4,5] which have leveraged this technology to enhance user experience and portability. Figure 1A illustrates the device configuration of a traditional pancake optics system, highlighting its key components. This optical setup keeps not only an outstanding image quality but also enables a compact form factor. By employing threefold light path folding within the pancake optics, these systems achieve a shorter focal length, thereby drastically reducing the overall volume. However, this approach faces a fundamental limitation—considerable light loss. As depicted in Figure 1B, only approximately 25% of the light emitted from the display panel reaches the observer's eye.

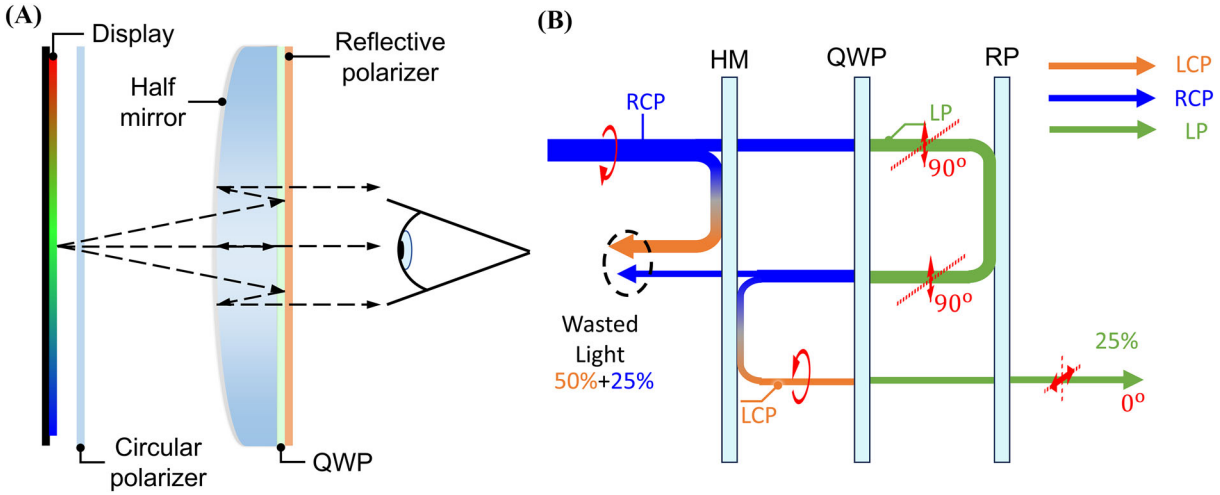

FIGURE 1 Scheme of conventional virtual reality (VR) pancake optics. (A) Device configuration and (B) basic working principle.

To address this challenge, various strategies have been proposed to enhance the optical efficiency. One such approach involves collimated backlighting[6,7] and optimizing pixel aspect ratio.[8] Additionally, utilizing hologram film and laser sources presents another promising avenue for improving efficiency.[9] Recently, a double-path pancake optics was proposed to double the optical efficiency. By recycling a portion of wasted light in the traditional pancake optics with cholesteric liquid crystal (CLC) reflectors[10] or another pair of reflective polarizer (RP) and quarter-wave plates (QWPs),[11] the optical efficiency limit can be improved to 50%.

In this paper, we will first give an overview of the state-of-the-art of previous pancake optics, including conventional pancake optics and double-path pancake optics. The major issues related to these designs will also be analyzed and discussed. Then, to overcome the fundamental limitation posed by the HM and to preserve substantial design flexibility, we propose a novel pancake optics solution that is theoretically lossless. This solution integrates a nonreciprocal polarization rotator between two RPs. To validate this concept, we conducted a preliminary experiment using readily available components. The experimental results align closely with our theoretical analyses, affirming the feasibility of our proposed approach. To achieve a full-color display, a multi-layer Faraday rotator (FR) design is discussed to achieve broadband performance. Additionally, to realize a large field of view (FoV) in VR displays, the angular response of terbium gallium garnet (TGG) FR is also simulated with the 4-by-4 matrix method for the first time. Finally, a potential application in near-infrared (NIR) night vision goggles is also discussed.

2 | OVERVIEW OF PREVIOUS PANCAKE OPTICS

The traditional pancake optics was originally proposed for flight simulators, and now, it has found renewed interest for compact VR headsets. Figure 1B depicts the operation mechanism of a conventional pancake optics system. More specifically, the emitted right-handed circularly polarized (RCP) light from the microdisplay panel keeps the following path: It goes through the HM, where 50% of the incident light is reflected and lost. The remaining 50% continues to the QWP and is converted into linearly polarized (LP) light. Once the LP light interacts with the RP, almost all the light is reflected toward the QWP and HM. In this process, the QWP converts LP light back to RCP light. When the RCP light encounters HM, another 25% passing through the HM, results in an additional loss. The remaining 25% of light is reflected and converted to left-handed circularly polarized (LCP) light due to the reverse of propagation direction and successfully passes through the QWP and RP. Ultimately, the optical path is folded three times in such pancake optics, but only about 25% of the light (assuming no other loss) from the display panel reaches the observer's eye. Due to the folding capability of the pancake optics, the optical power of the system is dramatically improved, thus the form factor is dramatically reduced. However, the low optical efficiency would require a much brighter microdisplay to achieve the same brightness, which in turn consumes more battery power and reduces the lifetime of microdisplays, especially micro-OLED. Another issue is the ghost images[12–14] introduced by the unperfect polarization

conversion in QWP, low contrast ratio of RP, unperfect alignment between QWP and LP, and so forth.

In the above traditional pancake optics system, there are at least 75% light wasted finally, wherein 25% light is RCP light and 50% light is LCP light. To effectively utilize the energy in the system, Luo et al.[10] proposed to add an LCP cholesteric liquid crystal (CLC L) reflector in front of HM to recycle the 25% LCP light. Besides, the RP and QWP in Figure 1B can also be replaced by an RCP CLC reflector (CLC R), and then we achieve the final structure of the pancake optics system as shown in Figure 2A. More specifically, due to its polarization selectivity property as shown in Figure 2B, that is, reflecting LCP light while allowing RCP light to pass through, the incident RCP light can pass through the CLC L. When the RCP light encounters the HM, 50% of light will pass through the HM and experience the same folding process as in the conventional pancake optics. Another 50% of light will be reflected and converted to LCP light due to the reverse of propagation. The LCP light will be reflected due to the polarization selectivity of CLC L. When it encounters the HM again, 25% of the light will be reflected and become wasted light. The remaining 25% of light will pass through HM and CLC R, finally going to the user's eyes. In this way, there are two different optical paths (images) in this system as shown in Figure 2C. To combine two images together and truly double the optical efficiency as shown in Figure 2D, the two optical paths are required to be the same, which indicates the lens design is symmetric with respect to the HM. Thus, such a requirement will increase the volume of the pancake lens compared to conventional one. And it will also significantly decrease the design freedom, especially for the multiple-piece pancake lens. One possible double-path pancake lens design with its essential optical elements is shown in Figure 2E. At the same time, Usukura et al.[11] also proposed a double-path pancake optics design, but with RPs and QWPs instead of CLC reflectors. However, the RP and QWP (especially QWP) are difficult to fabricate on a curved surface, which will further increase the

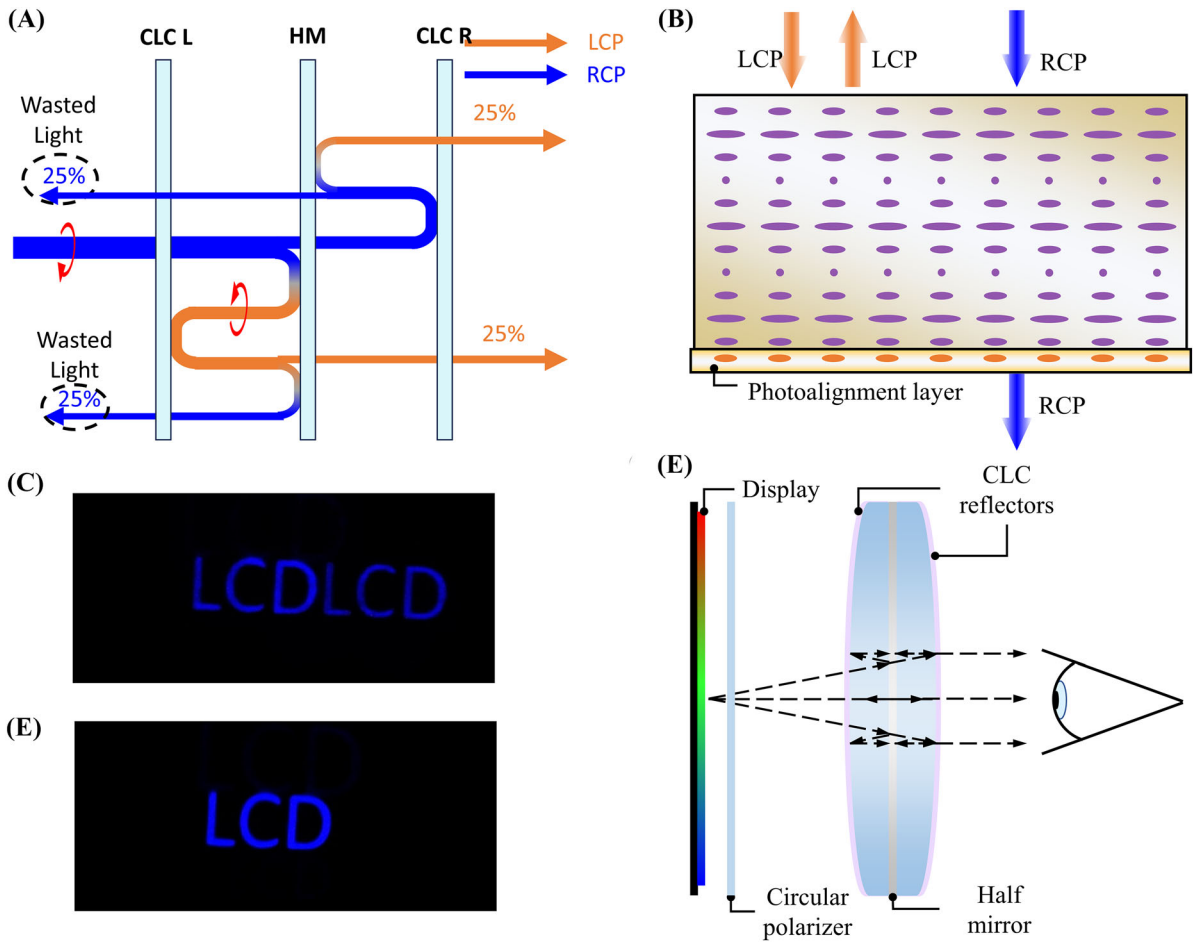

FIGURE 2 Double-path pancake optics. (A) Operation mechanism of double-path pancake optics system. (B) Polarization selectivity property of a left-handed circularly polarized (LCP) cholesteric liquid crystal (CLC L) reflector. Captured images from (C) tilted and (D) aligned double-path pancake optics system. (E) A possible configuration of the double-path pancake optics.

volume of the double-path pancake optics. Besides, more optical elements will also cause more ghost images. Moreover, this design still incurs at least 50% light loss due to the presence of the HM.

3 | LOSSLESS PANCAKE OPTICS WITH NONRECIPROCAL POLARIZATION ROTATOR

Before diving into our lossless pancake system, it is crucial to grasp the concepts of nonreciprocal polarization rotations.[15,16] When an LP light traverses in a medium, optical rotation occurs due to the disparity between its LCP and RCP components. This phenomenon, induced by a magnetic field along the wave propagation direction, is known as Faraday rotation or nonreciprocal polarization rotation. Specifically, the Faraday rotation angle, denoted by θ, is directly proportional to the magnetic field strength. More importantly, the rotation direction is determined solely by the magnetic field, irrespective of the optical wave's propagation direction as described in the following equation:

$$\theta(\lambda) = V(\lambda)BL, \tag{1}$$

where $V(\lambda)$ represents the Verdet constant of the material, B denotes the magnetic flux density along the propagation direction, and L signifies the length of the magneto-optical element. As illustrated in Figure 3A, the direction of polarization rotation remains consistent even when the propagation direction is reversed, which is referred to as nonreciprocal polarization rotation. Consequently, a roundtrip involving both forward and backward propagations leads to a cumulative rotation of 2θ.

In the following, we present a novel pancake optics structure[17] utilizing the nonreciprocal polarization rotator described earlier. The system configuration is depicted in Figure 3B. Our proposed pancake optics comprises a 45° FR sandwiched between two RPs with transmission axes inclined at 45° to each other. In an ideal scenario, LP light, such as horizontally polarized light from the microdisplay, initially traverses completely through the first RP. Subsequently, it encounters the FR, where it undergoes a 45° polarization rotation before being reflected by the second RP and redirected backward toward the FR due to the polarization selectivity of the RP. All light then passes through the FR, experiencing another 45° polarization rotation and emerging as vertically polarized. Under these conditions, the light reflects off the first RP, returning to the FR. It once again

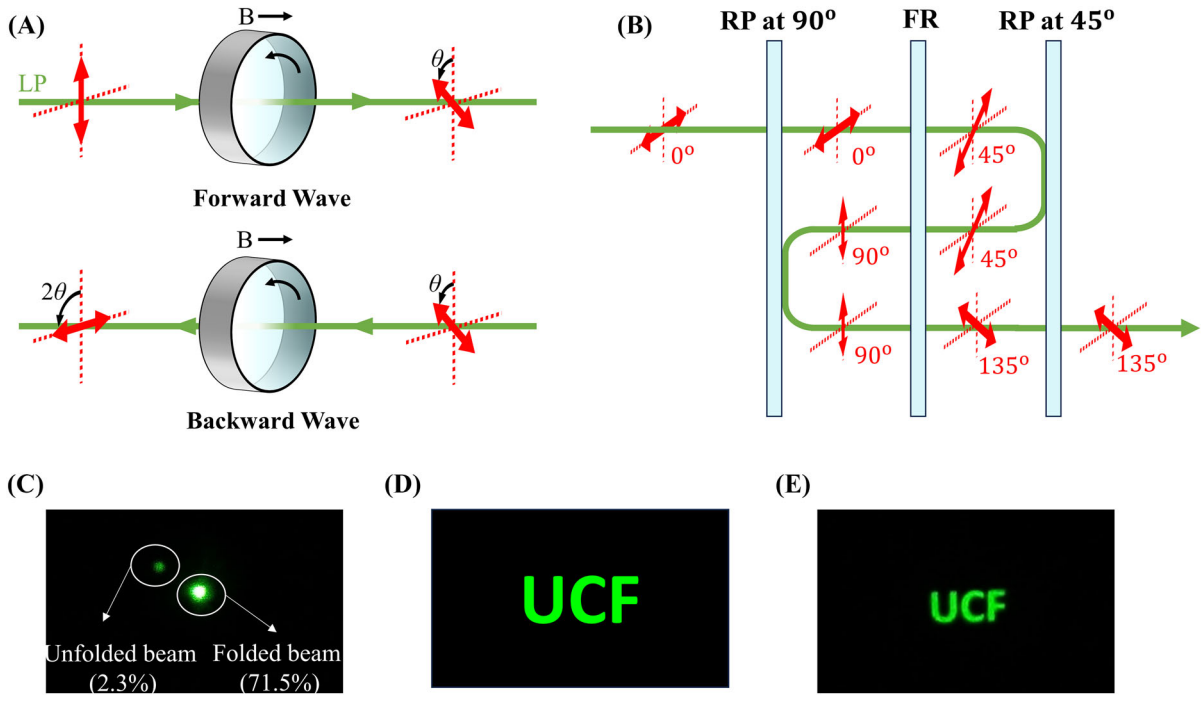

FIGURE 3 Scheme and experiments of the lossless virtual reality (VR) pancake optics. (A) Polarization rotation in a nonreciprocal polarization rotator through forward propagation and backward propagation. (B) Basic working principle of the lossless pancake optics system. (C) Captured images in the lossless pancake optics system with a laser source. (D) Original image from micro-OLED panel. (E) Captured images in the lossless pancake optics system with a micro-OLED panel.

traverses through the FR, undergoing a 45° polarization rotation, before passing through the second RP and reaching the user's eye. Importantly, throughout this entire process, there is no loss of light as all polarization rotations are achieved by the lossless FR. Furthermore, a lens can be inserted at any position, eliminating the necessity for a symmetric lens design in the previously mentioned double-path pancake system.

To validate our concept, we utilized a commercially available TGG crystal as the FR due to its large Verdet constant and minimal absorption in the visible spectral range. Additionally, two dual brightness enhancement films (DBEFs) served as the RPs. Initially, we aimed to confirm the optical efficiency of our system. We employed a 45° FR operating within the 510–550 nm range (sourced from Thorlabs). A 532-nm laser was positioned at 4 cm in front of the first RP, with a 5-cm separation between the two RPs. To facilitate the easier evaluation of different folded images, we intentionally enlarged the system volume, and the light source was inclined at a slight angle for this purpose. It is important to note that the objective of this experiment is to solely demonstrate the folding capability, and our breadboard pancake system did not possess any optical bending power.

Figure 3C illustrates the laser beams captured in the lossless pancake optics system. One can observe the energy is primarily concentrated in the folded beam (bright beam) and only a small part of the light is concentrated in the unfolded beam (weak beam). Based on our measurement, the folded beam contains around 71.5% energy, the unfolded beam contains 2.3% energy, and all other energy is reflected to the panel due to the unperfect RPs or absorbed by the FR.

Although our proposed pancake system exhibits a superior optical efficiency compared to conventional designs, it falls short of achieving the theoretical limit of 100%. To analyze the energy loss comprehensively, we must assess the performance of all optical elements involved.

Beginning with the DBEF RPs, in the block state, they typically exhibit approximately 99% reflectance and 1% transmittance, respectively. Conversely, in the pass state, these values are reversed. However, when laminated onto a glass substrate without an antireflection coating, their reflectance and transmittance in the block state are changed to about 98.4% and 1.6%, respectively, while in the pass state, they are about 8.5% and 91.5%. This substantial reduction in optical efficiency stems from the fact that the folded image undergoes reflection and transmission by the RPs twice. Another crucial element is FR, which is responsible for controlling the polarization rotation. The TGG FR typically exhibits an absorption of approximately 1%, with reflectance and transmittance of about 1% and 98% at 532 nm, respectively, according to Thorlabs' specifications. Overall, considering the parameters mentioned above, the optical efficiency is estimated to be approximately 76.3%. This value slightly exceeds our measured optical efficiency of 71.5%, with the ~5% difference possibly attributed to laser beam diffraction.

To enhance optical efficiency further, strategies such as applying an antireflection coating (<0.25%) on the substrate and utilizing high-performance RP films like 3M™ RPs[18] with 99.9% transmittance in the pass state and 99.9% reflectance in the block state can significantly boost the efficiency to around 93.2%, which is approximately four times higher than that of conventional pancake lenses.

In addition to the experiment using a green laser, we further explored our pancake systems utilizing a micro-OLED (organic light-emitting diode) panel. Figure 3D,E represents the original image sourced from the display panel and the images captured within the novel pancake optics systems employing a micro-OLED panel. As depicted in Figure 3E, the captured image appears smaller than the image displayed on the panel. This size reduction is attributed to the longer optical path in the experiment, where no bending optical power is utilized. Such a result aligns with our theoretical expectations.

To realize full-color display in VR displays, the FR should have a broadband spectral response. According to the specifications on the Thorlabs, the TGG FR used in our experiment only works for green light due to the dispersion of the Verdet constant in the following equation:

$$V(\lambda) = \frac{K}{\lambda_0^2 - \lambda^2}, \tag{2}$$

where $K = 4.45 * 10^7 \mathrm{rad\,nm^2\,T^{-1}\,m^{-1}}$ and $\lambda_0 = 258.2\,nm$ is the effective transition wavelength. For most FR materials, the Verdet constant decreases (in absolute value) with increasing wavelength; for TGG it is equal to 206 $\mathrm{rad\,T^{-1}\,m^{-1}}$ at $\lambda = 532\,\mathrm{nm}$ and 134 $\mathrm{rad\,T^{-1}\,m^{-1}}$ at $\lambda = 632\,\mathrm{nm}$. These characteristics limit the operation spectrum of FR to a narrow range. However, to enable the proposed pancake system to display full-color images, a broadband FR is necessary. To achieve broadband FR functionality in both forward and backward directions, a solution involving the combination of multiple FRs and QWPs has been proposed and realized.[19]

Besides, to achieve a large FoV in VR displays, the employed FR should have a wide angular response. However, the angular response of FR has not been investigated previously because its major applications are for

laser beams. To simulate the angular response of a FR, the permittivity tensor is needed. Here, we first introduce the method of calculating the permittivity tensor of magneto-optic material (or gyromagnetic material) and then simulate the angular response with the 4-by-4 matrix method.[20]

As discussed previously, in a magneto-optic material, the presence of a magnetic field can change the permittivity tensor of the material. Without considering the loss, the tensor becomes anisotropic with complex off-diagonal components as shown in the following equation:

$$\varepsilon = \begin{bmatrix} \varepsilon_1 & +ig & 0 \\ -ig & \varepsilon_1 & 0 \\ 0 & 0 & \varepsilon_2 \end{bmatrix}. \tag{3}$$

Fundamentally, the tensor could be described and derived by the Lorentzian model or a linearized Landau–Lifshitz–Gilbert (saturated dipole) model.[21,22] However, if we know the Verdet constant and the average refractive index ($n_{avg} = (n_{LCP} + n_{RCP})/2$) of the magneto-optic material, then the tensor can be calculated more easily as follows.

To obtain the tensor, we need to know the circular birefringence Δn of the FR, which can be described by

$$\Delta n = n_{LCP} - n_{RCP}, \tag{4}$$

where n_{LCP} and n_{RCP} represent the refractive index of the LCP light and RCP light, respectively. Since the LCP and RCP light is a set of orthonormal basis, any LP light with an angle θ with respect to the x-axis can be described by the superposition of LCP $\left(E_{LCP} = \frac{\sqrt{2}}{2}(\hat{x} + i\hat{y})\right)$ and RCP $\left(E_{RCP} = \frac{\sqrt{2}}{2}(\hat{x} - i\hat{y})\right)$ light as follows:

$$E_\theta = \frac{\sqrt{2}}{2}\left(e^{-i\theta}E_{LCP} + e^{i\theta}E_{RCP}\right) = \cos(\theta)\hat{x} + \sin(\theta)\hat{y}. \tag{5}$$

After passing through an FR with a rotation angle of $\Delta\theta$, an additional phase difference $2\Delta\theta$ between LCP and RCP light will be introduced and the LP light will rotate $\Delta\theta$ as described in the following:

$$\begin{aligned} E_{out} &= \frac{\sqrt{2}}{2}\left(e^{-i\theta}e^{-i\Delta\theta}E_{LCP} + e^{i\theta}e^{+i\Delta\theta}E_{RCP}\right) \\ &= \cos(\theta + \Delta\theta)\hat{x} + \sin(\theta + \Delta\theta)\hat{y}. \end{aligned} \tag{6}$$

If the thickness of the FR is L, then an additional phase difference is accumulated by the propagation phase:

$$2\Delta\theta = k_0 * \Delta n * L, \tag{7}$$

where k_0 corresponds to the wave vector of the incident light in a vacuum.

Here, taking the TGG material as an example, the circular birefringence Δn can be calculated based on Equations (1), (2), and (7). Besides, the average refractive index n_{avg} of TGG has been measured previously.[23] Using these two parameters Δn and n_{avg}, the refractive index of LCP and RCP light can be derived as follows:

$$n_{LCP} = \frac{2n_{avg} + \Delta n}{2}, \tag{8}$$

$$n_{RCP} = \frac{2n_{avg} - \Delta n}{2}. \tag{9}$$

Therefore, we achieve the permittivity tensor ε_{CP} in the circular polarization basis as shown below:

$$\varepsilon_{CP} = \begin{bmatrix} n_{LCP}^2 & 0 & 0 \\ 0 & n_{RCP}^2 & 0 \\ 0 & 0 & n_{avg}^2 \end{bmatrix}. \tag{10}$$

Simply, by changing the basis from circularly polarized light to LP light with the unitary matrix U, the permittivity tensor ε in LP light basis can be expressed as:

$$\begin{aligned} \varepsilon &= U\varepsilon_{CP}U^\dagger \\ &= \begin{bmatrix} \frac{1}{\sqrt{2}} & \frac{1}{\sqrt{2}} & 0 \\ -\frac{1}{\sqrt{2}}\mathrm{i} & \frac{1}{\sqrt{2}}\mathrm{i} & 0 \\ 0 & 0 & 1 \end{bmatrix} \begin{bmatrix} n_{LCP}^2 & 0 & 0 \\ 0 & n_{RCP}^2 & 0 \\ 0 & 0 & n_{avg}^2 \end{bmatrix} \begin{bmatrix} \frac{1}{\sqrt{2}} & \frac{1}{\sqrt{2}}\mathrm{i} & 0 \\ \frac{1}{\sqrt{2}} & -\frac{1}{\sqrt{2}}\mathrm{i} & 0 \\ 0 & 0 & 1 \end{bmatrix} \\ &= \begin{bmatrix} \frac{(n_{LCP}^2 + n_{RCP}^2)}{2} & i\frac{(n_{LCP}^2 + n_{RCP}^2)}{2} & 0 \\ -i\frac{(n_{LCP}^2 + n_{RCP}^2)}{2} & \frac{(n_{LCP}^2 + n_{RCP}^2)}{2} & 0 \\ 0 & 0 & n_{avg}^2 \end{bmatrix}. \end{aligned} \tag{11}$$

Once we obtain the permittivity tensor, the angular response can be easily simulated by the 4-by-4 matrix or extended Jones matrix methods. Here, the angular response of TGG FR is simulated by the 4-by-4 matrix method. Assuming the magnetic field flux is 1 T and the central wavelength of TGG FR is 525 nm. To achieve a 45° rotation angle, the required thickness is L ≈ 3.688 mm. To ensure the accuracy of the simulation result, the spectral response is simulated by both the 4-by-4 and Jones matrix as shown in Figure 4A. From Figure 4A, these two methods match very well.

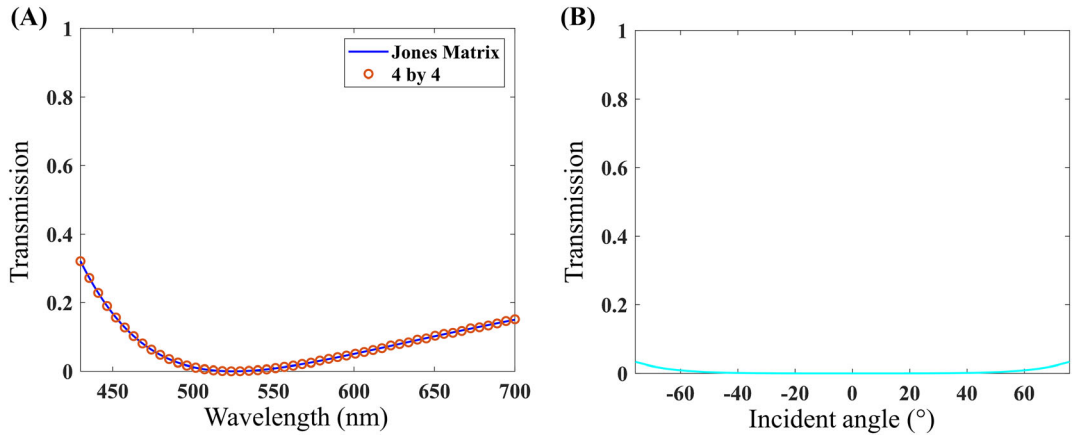

FIGURE 4 Simulation of angular and spectral performance of a terbium gallium garnet (TGG) Faraday rotator (FR). (A) Spectral response of FR with a rotation angle of 45° at central wavelength 525 nm with Jones matrix and 4-by-4 matrix methods. (B) Angular response of FR with a rotation angle of 45° at central wavelength 525 nm with the 4-by-4 matrix method.

Furthermore, the angular response at central wavelength $\lambda = 525$ nm is investigated as shown in Figure 4B. More importantly, the FR is basically inert to the incident angle within the $\pm 60°$ range, which can dramatically improve the contrast ratio of our lossless pancake optics design.

4 | DISCUSSION

The development of lossless pancake optics encounters numerous challenges stemming from the limited options of magneto-optical materials at the present time. The primary challenge lies in achieving a thin-film FR. To achieve this, two key aspects are essential. Firstly, the material must possess a large Verdet constant in the visible region. While TGG already exhibits a relatively large Verdet constant in this range, it remains insufficient to enable a thin-film form factor. Extensive research[24,25] has been dedicated to exploring materials with a large Verdet constant. For instance, recent research[26] has uncovered a class of organic materials with a remarkable Verdet constant of nearly 8×10^4 rad T^{-1} m^{-1} at 520 nm. This Verdet constant is approximately 360 times larger than that of TGG crystal, suggesting that a thin film made from such a material could be 360 times thinner than TGG.

Furthermore, the effective aperture of commercial TGG crystals is often limited, typically around 5 mm, due to the fringe field effect of external magnets. Such a small effective aperture inevitably results in a relatively narrow FoV. Hence, the choice of magnetic field source is crucial. As indicated in Equation (1), magnetic fields can be generated by a solenoid, external magnets, or a magnetized material itself (bias-magnet-free FR). However, the first two methods might be too bulky and heavy to support a large FoV for a compact and lightweight VR headset. Moreover, the fringe field effect associated with these methods further reduces the effective aperture of the FR, leading to a smaller FoV.

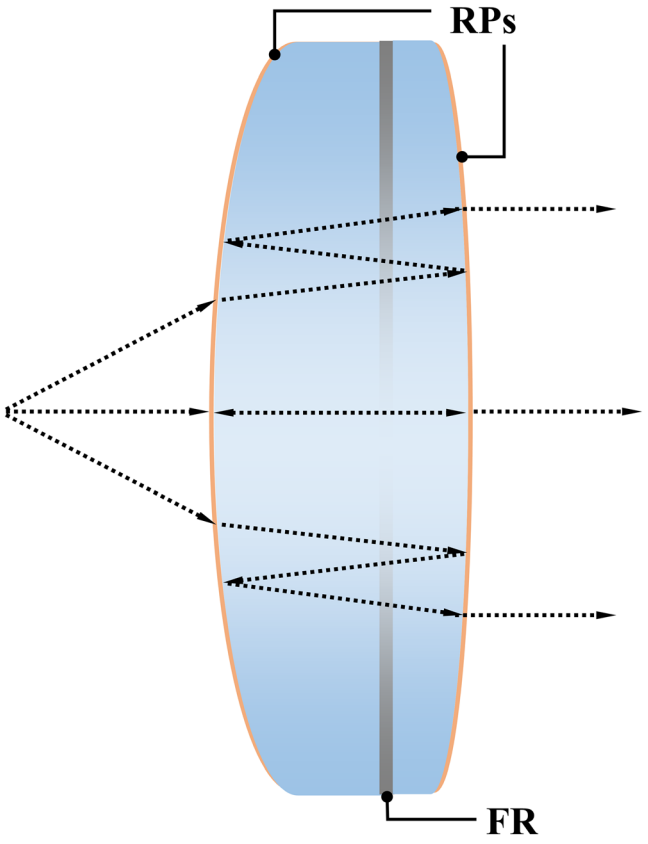

FIGURE 5 One possible lossless pancake lens design for near-infrared (NIR) night vision goggles.

The ideal FR should be a magnetless thin film with a large effective area. Magnetless thin films (measuring

20 mm × 20 mm × 480 μm) of magnetization latching bismuth-substituted rare-earth iron garnets[27,28] (BIG) are now commercially available from Coherent. However, the BIG FR primarily operates in the NIR region due to its significant absorption in the visible range. Consequently, our novel pancake optics system, demonstrated with a thin-film BIG FR, is also suitable for certain NIR imaging applications. One promising application is an objective lens for night vision goggles, which demands a compact form factor and NIR operation.[29] In such applications, the thin-film BIG FR and NIR wire-grid polarizers can be effectively employed in pancake optics to drastically reduce the form factor of night vision goggles. A possible lens design is illustrated in Figure 5.

5 | CONCLUSION

In this paper, we initially introduce the working principles, pros, and cons of conventional and double-path pancake optics designs. To enhance the optical efficiency and shrink the form factor of pancake optics, we propose and demonstrate a novel pancake optics system utilizing a nonreciprocal polarization rotator sandwiched between two RPs. This design overcomes the efficiency limitations of traditional pancake optics systems while maintaining a compact form factor similar to conventional pancake optics. Our measured optical efficiency is 71.5%, which is approximately 5% lower than the calculated value. By further applying AR coating to the optical components and utilizing higher-quality RPs, we anticipate raising the optical efficiency to about 93.2%. Additionally, to achieve full-color and wide FoV VR displays, the spectral and angular response of TGG FR is simulated using the Jones matrix and 4-by-4 matrix methods. Furthermore, the challenges and potential applications of lossless pancake optics in VR and night vision goggles are discussed from a material perspective. Overall, these demonstrations highlight the potential for the novel pancake optics system to revolutionize next-generation VR displays, offering lightweight, compact form factors, and low power consumption. Moreover, the urgent need for a thin-film FR that is both magnetless and highly transparent, while possessing a large Verdet constant in the visible region, is expected to drive future advancements in magneto-optic material development.

ACKNOWLEDGMENTS

The UCF group is indebted to Dr. Yu-Hsin Huang of AUO Corporation for providing the DBEF films.

ORCID

Shin-Tson Wu https://orcid.org/0000-0002-0943-0440

REFERENCES

1. Kress BC. Optical architectures for augmented-, virtual-, and mixed-reality headsets Bellingham: SPIE Press; 2020.
2. Ding Y, Yang Q, Li Y, Yang Z, Wang Z, Liang H, et al. Waveguide-based augmented reality displays: perspectives and challenges. eLight. 2023;3(1):24. https://doi.org/10.1186/s43593-023-00057-z
3. Xiong J, Hsiang EL, He Z, Zhan T, Wu ST. Augmented reality and virtual reality displays: emerging technologies and future perspectives. Light Sci Appl. 2021;10(1):216. https://doi.org/10.1038/s41377-021-00658-8
4. LaRussa JA, Gill AT. The holographic pancake window TM. In: Beiser L, editor. Proc SPIE 0162; 1978. p. 120–9.
5. Li Y, Zhan T, Yang Z, Xu C, LiKamWa PL, Li K, et al. Broadband cholesteric liquid crystal lens for chromatic aberration correction in catadioptric virtual reality optics. Opt Express. 2021;29(4):6011–20. https://doi.org/10.1364/OE.419595
6. Zou J, Zhan T, Hsiang EL, Du X, Yu X, Li K, et al. Doubling the optical efficiency of VR systems with a directional backlight and a diffractive deflection film. Opt Express. 2021;29(13):20673–86. https://doi.org/10.1364/OE.430920
7. Hsiang EL, Yang Z, Zhan T, Zou J, Akimoto H, Wu ST. Optimizing the display performance for virtual reality systems. OSA Continuum. 2021;4(12):3052–67. https://doi.org/10.1364/OSAC.441739
8. Wu YH, Tsai CH, Wu YH, Cherng YS, Tai MJ, Huang P, et al. 5-2: invited paper: high dynamic range 2117-ppi LCD for VR displays. In: SID Symposium Digest of Technical Papers 54(1); 2023. p. 36–9.
9. Komura S, Okuda K, Kijima H. 49-4: thin and lightweight head-mounted displays with polarized laser backlights and holographic optics. In: SID Symposium Digest of Technical Papers 53(1); 2022. p. 636–9.
10. Luo Z, Ding Y, Rao Y, Wu ST. High-efficiency folded optics for near-eye displays. J Soc Inf Disp. 2023;31(5):336–43. https://doi.org/10.1002/jsid.1207
11. Usukura N, Minoura K, Maruyama R. Novel pancake-based HMD optics to improve light efficiency. J Soc Inf Disp. 2023;31(5):344–54. https://doi.org/10.1002/jsid.1212
12. Geng Y, Gollier J, Wheelwright B, Peng F, Sulai Y, Lewis B, et al. Viewing optics for immersive near-eye displays: pupil swim/size and weight/stray light. Proc SPIE. 2018;10676:19–35.
13. Hou Q, Cheng D, Li Y, Zhang T, Li D, Huang Y, et al. Stray light analysis and suppression method of a pancake virtual reality head-mounted display. Opt Express. 2022;30(25):44918–32. https://doi.org/10.1364/OE.476078
14. Cheng D, Hou Q, Li Y, Zhang T, Li D, Huang Y, et al. Optical design and pupil swim analysis of a compact, large EPD and immersive VR head mounted display. Opt Express. 2022;30(5):6584–602. https://doi.org/10.1364/OE.452747
15. Saleh BEA, Teich MC. Fundamentals of photonics John Wiley & Sons; 2019.
16. Inoue M, Levy M, Baryshev AV. Magnetophotonics: from theory to applications [Internet]. Berlin, Heidelberg: Springer; 2013. (Springer Series in Materials Science). Available from: https://doi.org/10.1007/978-3-642-35509-7
17. Ding Y, Luo Z, Borjigin G, Wu ST. Breaking the optical efficiency limit of virtual reality with a nonreciprocal polarization

rotator. Opto-Electron Adv. 2024;7(3):230178. https://doi.org/10.29026/oea.2024.230178
18. Le J, Hao B, Aastuen D, Kent S, Kotz A, O'Neill M, et al. High resolution reflective polarizer lens for catadioptric VR optics with accommodating eye box design. Proc SPIE. 2023;12449:124–33.
19. Berent M, Rangelov AA, Vitanov NV. Broadband Faraday isolator. J Opt Soc am a. 2013;30(1):149–53. https://doi.org/10.1364/josaa.30.000149
20. Huang YH, Wu TX, Wu ST. Simulations of liquid-crystal Fabry-Perot etalons by an improved 4x4 matrix method. J Appl Phys. 2003;93(5):2490–5. https://doi.org/10.1063/1.1542652
21. Pershan PS. Magneto-optical effects. J Appl Phys. 1967;38(3):1482–90. https://doi.org/10.1063/1.1709678
22. Haider T. A review of magneto-optic effects and its application. Int J Electromagn Appl. 2017;7(1):17–24.
23. Schlarb U, Sugg B. Refractive index of terbium gallium garnet. Phys Status Solidi (b). 1994;182(2):K91–3.
24. Nelson Z, Delage-Laurin L, Swager TM. ABCs of Faraday rotation in organic materials. J am Chem Soc. 2022;144(27):11912–26. https://doi.org/10.1021/jacs.2c01983
25. Carothers KJ, Norwood RA, Pyun J. High verdet constant materials for magneto-optical Faraday rotation: a review. Chem Mater. 2022;34(6):2531–44. https://doi.org/10.1021/acs.chemmater.2c00158
26. Vandendriessche S, Van Cleuvenbergen S, Willot P, Hennrich G, Srebro M, Valev VK, et al. Giant Faraday rotation in mesogenic organic molecules. Chem Mater. 2013;25(7):1139–43. https://doi.org/10.1021/cm4004118
27. Levy M. Nanomagnetic route to bias-magnet-free, on-chip Faraday rotators. J Opt Soc Am B. 2005;22(1):254–60. https://doi.org/10.1364/josab.22.000254
28. Karki D, Stenger V, Pollick A, Levy M. Thin-film magnetless Faraday rotators for compact heterogeneous integrated optical isolators. J Appl Phys. 2017;121(23):233101. https://doi.org/10.1063/1.4986237
29. Fein H, Ponting M. Design and fabrication toward a shorter, lightweight night vision goggle objective assembly with a nanolayered polymer gradient refractive index lens. In: 2017 Conference on Lasers and Electro-Optics (CLEO) IEEE; 2017. p. 1–2.

AUTHOR BIOGRAPHIES

Yuqiang Ding received his BS degree in Optical Engineering from Shandong University in 2021. He is currently working toward a PhD degree from the College of Optics and Photonics, University of Central Florida. His current research interests include novel liquid crystal optical elements and optical system design in near-eye displays.

Zhenyi Luo received his BE degree from the Department of Precision Instrument at Tsinghua University, China, and his MS degree from the Department of Chemistry at the University of Tokyo, Japan. Now he is a Ph.D. student at the College of Optics and Photonics, University of Central Florida. His research interests include advanced augmented reality and virtual reality displays, and novel liquid crystal devices.

Garimagai Borjigin received his BS in Engineering from Beijing Institute of Technology, China, and his Ph.D. in Engineering from the University of Tsukuba, Ibaraki, Japan. He is currently a postdoc fellow at the University of Tsukuba, Japan. His research interests include 3D displays, augmented reality, and virtual reality.

Shin-Tson Wu is a Trustee Chair professor at the College of Optics and Photonics, University of Central Florida (UCF). He is an Academician of Academia Sinica, a Charter Fellow of the National Academy of Inventors, and a Fellow of the IEEE, OSA, SID, and SPIE. He is a recipient of the Optica Edwin H. Land Medal (2022), SPIE Maria Goeppert-Mayer Award (2022), Optica Esther Hoffman Beller Medal (2014), SID Slottow-Owaki Prize (2011), Optica Joseph Fraunhofer Award (2010), SPIE G. G. Stokes Award (2008), and SID Jan Rajchman Prize (2008). In the past, he served as the founding Editor-In-Chief of the Journal of Display Technology, Optica publications council chair and board member, and SID honors and awards committee chair.

How to cite this article: Ding Y, Luo Z, Borjigin G, Wu S-T. High-efficiency and ultracompact pancake optics for virtual reality. J Soc Inf Display. 2024;32(5):341–9. https://doi.org/10.1002/jsid.1298